ISART 2011
Boulder, CO

Radar Adaptive Interference Mitigation

William L. Melvin, Ph.D.
Sensors & Electromagnetic Applications Laboratory
Georgia Tech Research Institute
(404)-407-8274, bill.melvin@gtri.gatech.edu

Outline

- Objectives
- Radar signal processing and DoFs
- Key example: array processing
- Adaptive architectures
- Wideband arrays
- Example results
- Summary
- References

Objectives

- Understand the basics of adaptive interference mitigation for radar
- Highlight the fundamental radar measurements and their utility in interference suppression
- Describe typical canceller architectures
- Consider spatial nulling as a primary example

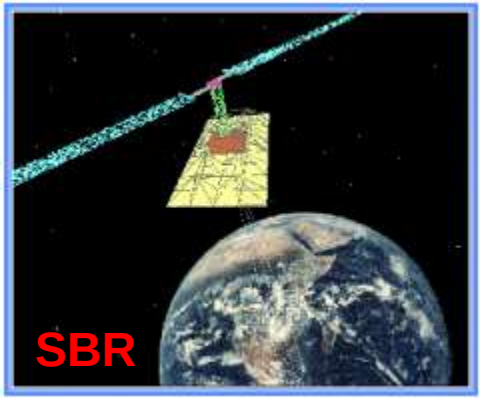

Radar Signal Processing

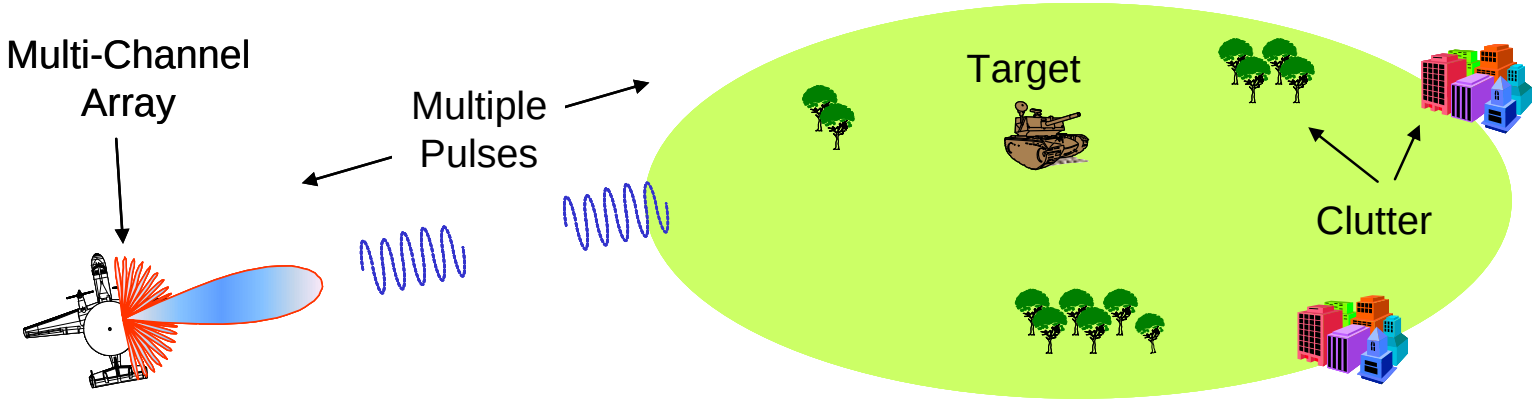

Combine thousands of voltages collected using pulsed, multichannel sensor to detect moving targets or image fixed targets → sophisticated algorithms generate the radar product

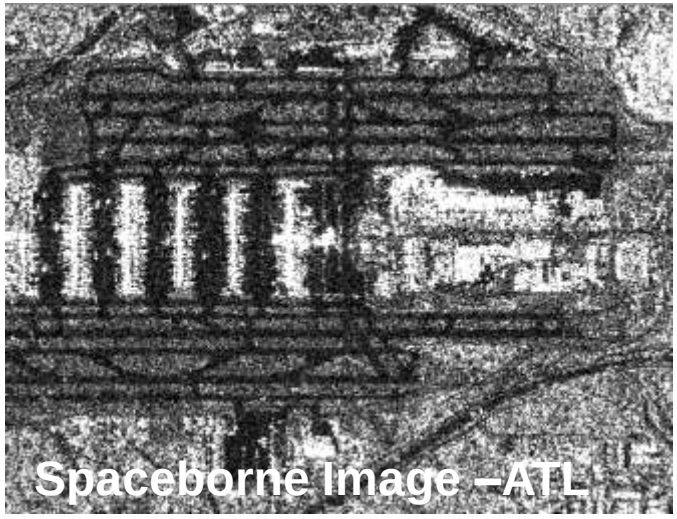

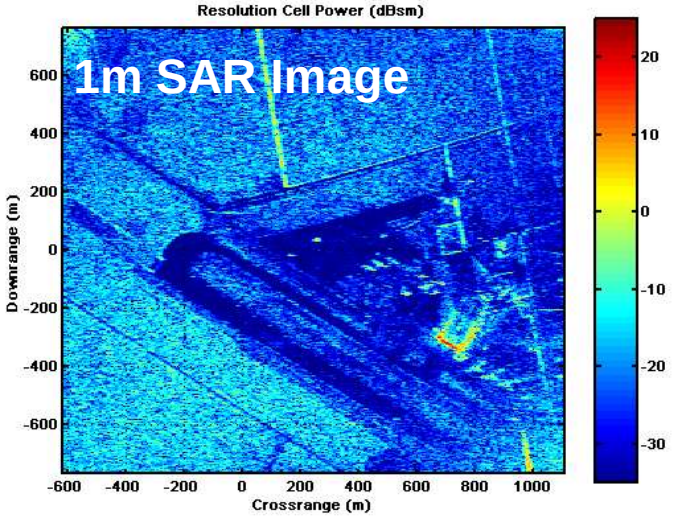

Radar Measurements

- Amplitude
  - Fast-time → generally, basis for detection
  - Slow-time → indicates target Doppler frequency
  - Spatial → indicates target direction of arrival
- Time-delay
  - Fast-time → range
  - Slow-time → variation yields Doppler frequency
  - Spatial → variation yields spatial frequency or direction or arrival
- Polarization
  - Linear → HH, VV, HV (VH reciprocal for passive targets)
  - Circular → LR, LL, RR (RL reciprocal for passive targets)
- Multi-scan
  - Non-coherent → clutter map
  - Coherent → change detection

Exploiting the radar measurement space is the key to improved detection and imaging

Processing Flow Diagram

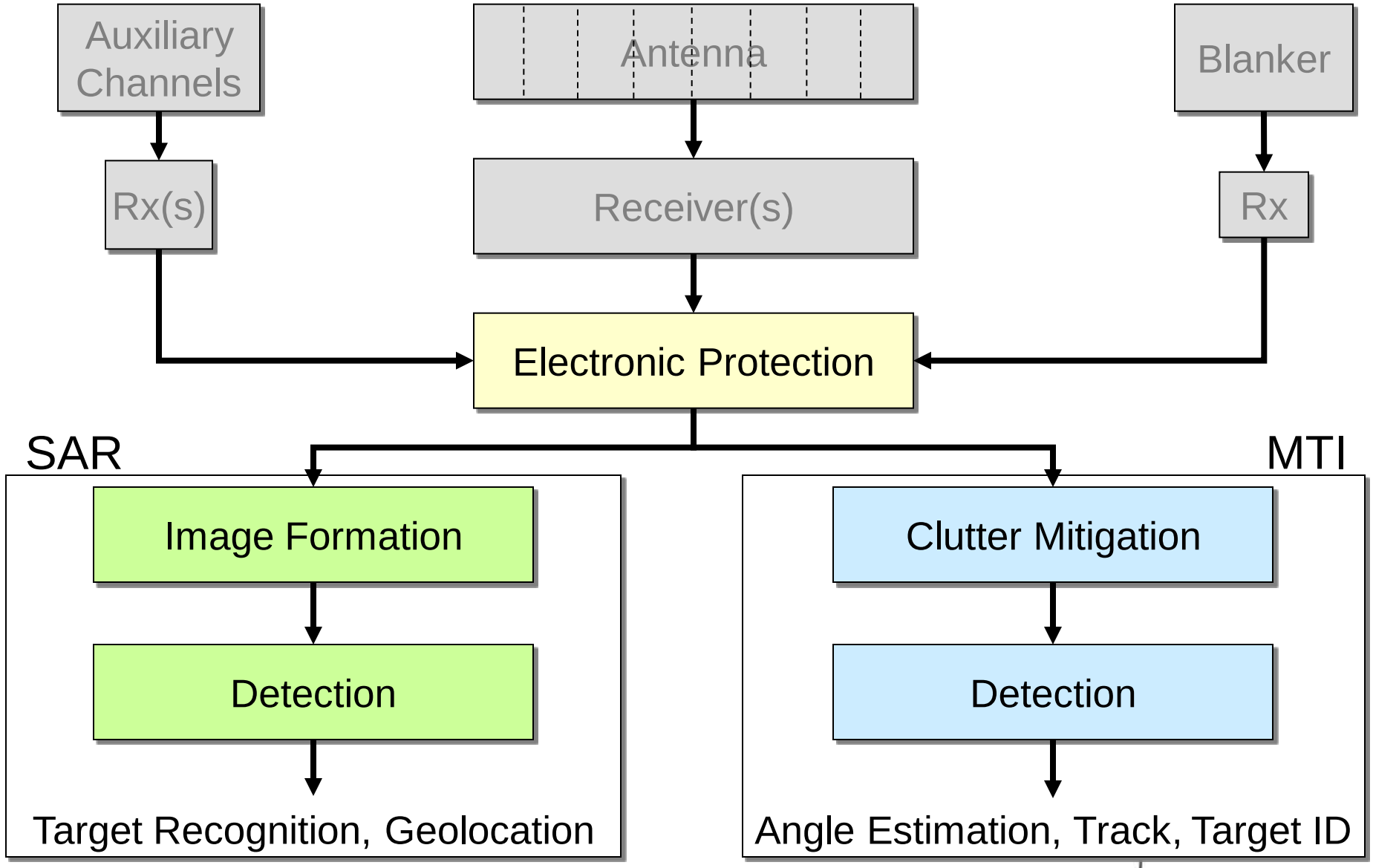

Signal-to-Noise Ratio (SNR) [1]

$$SNR(\phi,\theta) = \left(\frac{P_t G_t(\phi,\theta)}{4\pi r^2}\right)\left(\frac{\sigma_T}{4\pi r^2}\right)\left(\frac{A_e}{N_{in}\ F_n\ L_{rf}}\right)G_{sp}$$

P_t = Peak Power

G_t = Aperture Power Gain

ϕ,θ = Azimuth and Elevation Angle

r = Slant Range

σ_T = Target Radar Cross Section

A_e = Effective Receive Antenna Area

N_{in} = Input Receiver Noise

F_n = Noise Figure

L_{rf} = RF Losses

G_{sp} = Signal Processing Gains

- Radar range equation
  - Approximation
- Signal-to-noise ratio (SNR) characterizes detection performance
  - Noise assumed white Gaussian
- Key parameters are…
  - Power
  - Aperture terms
  - System temperature
    - Noise figure times standard temperature (290K)

For a fixed false alarm rate, probability of detection is a monotonic function of SNR

Detection in Colored-Noise [2-3]

- Besides providing adequate power-aperture product, the aerospace radar system design must incorporate…
  - A mechanism to suppress ground clutter returns
  - Jammer suppression capability
- Collectively we refer to clutter and jamming signals as *interference*
- Detection performance depends on the signal-to-interference-plus-noise ratio (SINR) and specified false-alarm rate (threshold)
  - SINR = SNR x clutter loss factor x jammer loss factor
  - Also, SINR <= SNR

• Interference-limited detection performance always less than noise-limited capability
• Drives system cost and complexity

Radar Detection: Common Observances

- P_D and P_{FA} move together
  - E.g., As the threshold decreases, P_D and P_{FA} both increase
- Decision rule operates in regions of conditional density overlap in an "optimal" fashion

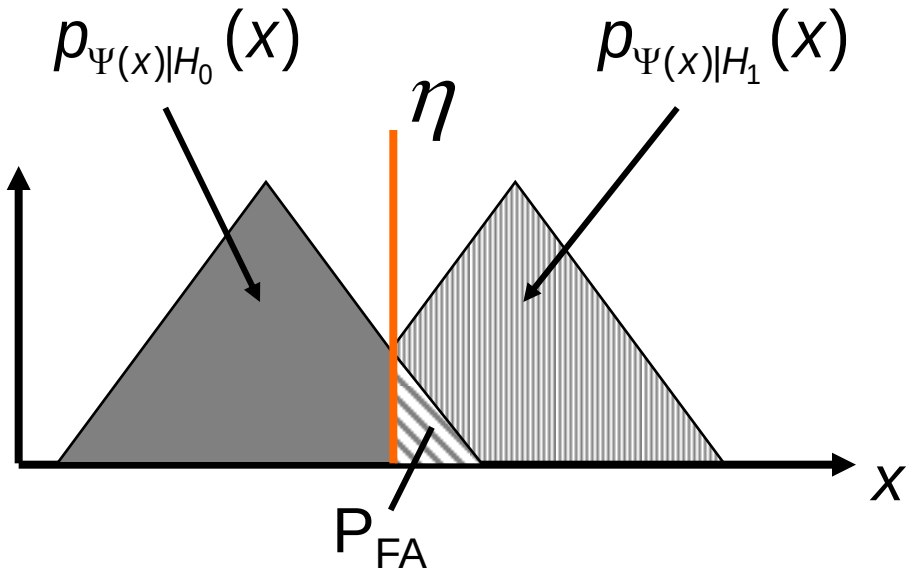

Larger SNR decreases overlap

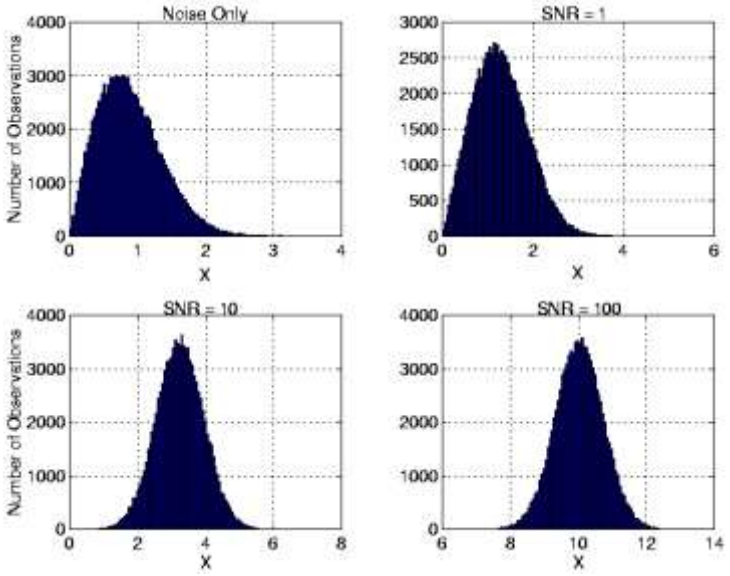

* Applies for white or colored noise

Receiver Operating Characteristic (ROC)

Non-Fluctuating Target

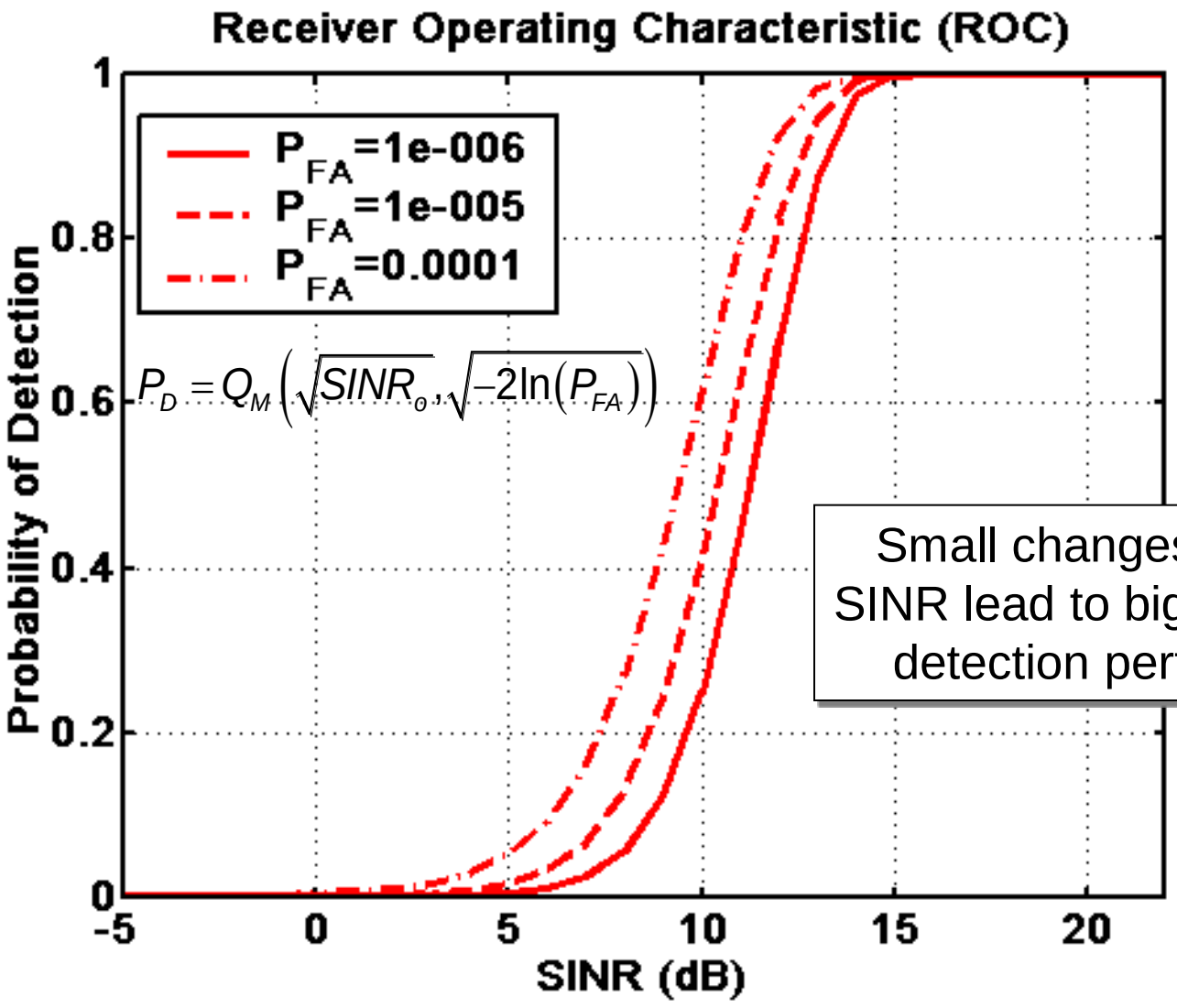

Small changes in output SINR lead to big changes in detection performance

Signal Diversity Enhances Detection

- Spatial and temporal signal diversity enhances radar detection performance
  - Signal diversity enables discrimination between target and interference
- Domains of interest…
  - Spatial domain (angle) -> multi-channel array antenna
  - Slow-time domain (Doppler) -> multi-pulse aperture
  - Fast-time domain (range) -> sample at 1/Bandwidth
- Clutter exhibits coupling in angle and Doppler
  - Differences between clutter and target angle-Doppler responses enables detection
    - Ground moving target indication (GMTI)
- Narrowband noise jamming is correlated in angle, white in Doppler
- Wideband jamming and jammer multipath correlated in angle and fast-time

Signal Diversity Enhances Detection Performance [4-9]

$$\mathbf{x_k} = \begin{bmatrix} \mathbf{x_{k/x}}(y_1, z_1) \\ \mathbf{x_{k/x}}(y_2, z_1) \\ \vdots \\ \mathbf{x_{k/x}}(y_N, z_1) \\ \mathbf{x_{k/x}}(y_1, z_2) \\ \vdots \\ \mathbf{x_{k/x}}(y_N, z_2) \\ \vdots \\ \mathbf{x_{k/x}}(y_1, z_P) \\ \vdots \\ \mathbf{x_{k/x}}(y_N, z_P) \end{bmatrix} \in C^{MNPx1}$$

"primary" observation

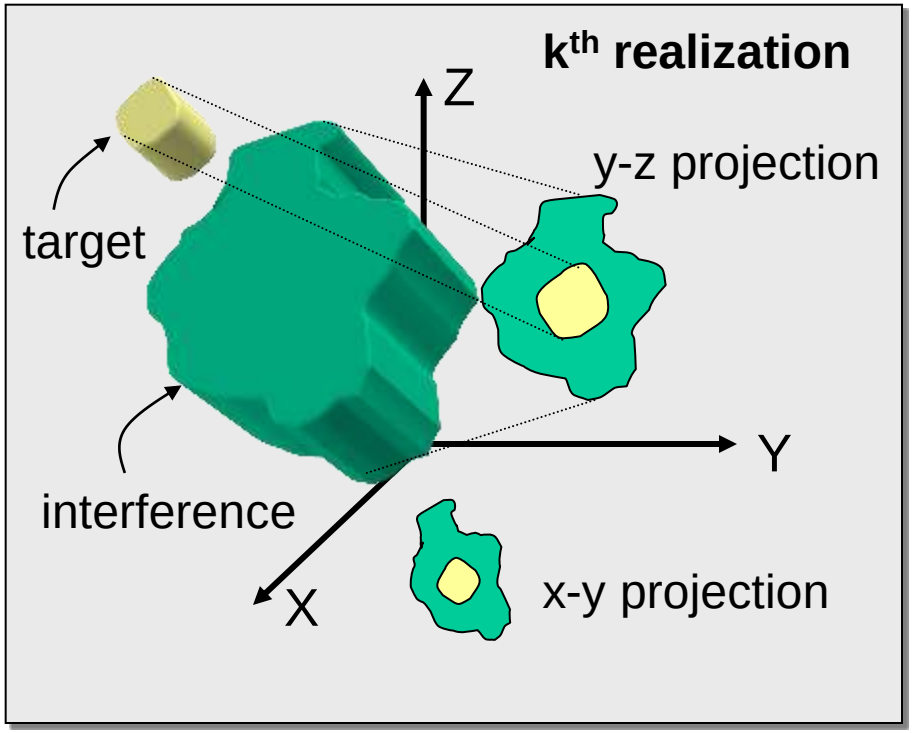

$$\xi_k = f\left(\mathbf{w_k^H x_k}\right) \underset{H_0}{\overset{H_1}{\gtrless}} T_k$$

decision statistic

weight vector

observation vector

decision threshold

Summary of Key Metrics

Metric	Definition	Comments
Signal-to-noise ratio (SNR)	Ratio of signal power to noise power	Noise is uncorrelated, white Gaussian; input SNR at pulse and element level; output SNR includes integration gain and weighting
Signal-to-interference-plus-noise ratio (SINR)	Ratio of signal power to interference plus noise power	Interference is colored noise, exhibits frequency preference; integration gain depends on interference type
SINR Loss	Ratio of SINR values under varying circumstances (usually between 0 and 1)	Common definitions include ratio of (1) maximum output SINR to SNR, (2) output SINR between adaptive and optimal filters
Improvement Factor (IF)	Ratio of output SINR to single element input SINR	Characteristic similar to definition #(1) defined in above line
Probability of Detection (P_D)	Probability correctly choose alternative hypothesis	Increases monotonically with output SINR
Probability of False Alarm (P_{FA})	Probability choose alternative hypothesis when null hypothesis is correct	High false alarm rate degrades tracking performance, overwhelms computing resources, biases CFAR detection threshold

Summary of Key Metrics (Continued)

Metric	Definition	Comments
Clutter-to-noise ratio (CNR)	Ratio of clutter power to noise power	Calculated at input or output, integration depends on sampling characteristics
Jammer-to-noise ratio (JNR)	Ratio of jammer power to noise power	Calculated at input or output, generally exhibits spatial integration gain
Signal-to-clutter ratio (SCR)	Ratio of SNR to CNR	Calculated at input or output, suggests detection performance potential
RMS Angle Error	Root mean square value of difference between true and estimated target bearing	Generally varies in proportion to the inverse square root of the output SINR
RMS Doppler Error	Root mean square value of difference between true and estimated target Doppler	Generally varies in proportion to the inverse square root of the output SINR
Floating Point Operations Per Second (FLOPS)	Number of floating point operations for complex arithmetic	Influenced strongly by particular implementation

Optimal Filter and Detector

- An optimal filter meets a specified goals
  - E.g., maximize output SINR
  - E.g., minimize output power subject to a set of constraints
- Its implementation is generally data-dependent

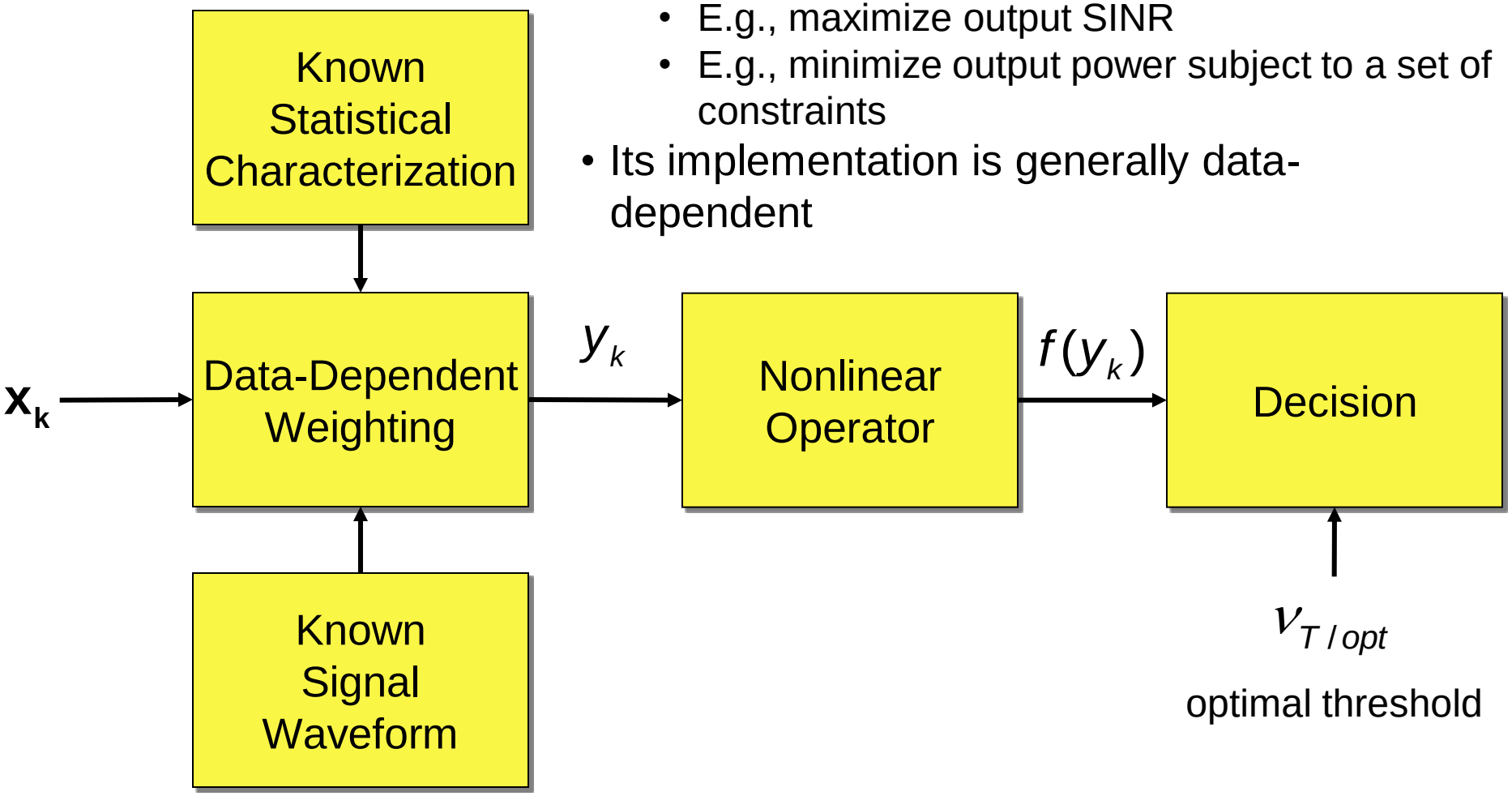

Adaptive Vs. Optimal [10-11]

- STAP is the data-domain implementation of the optimum filter
  - Statistics and target steering vector are unknowns

Optimum → Adaptive

Known Covariance Matrix → Estimated Covariance Matrix

Known Target Waveform → Hypothesized Steering Vector

Optimal Weight Vector → Adaptive Weight Vector

Spatial Sampling for Digital Beamforming

Uniform linear array (ULA)

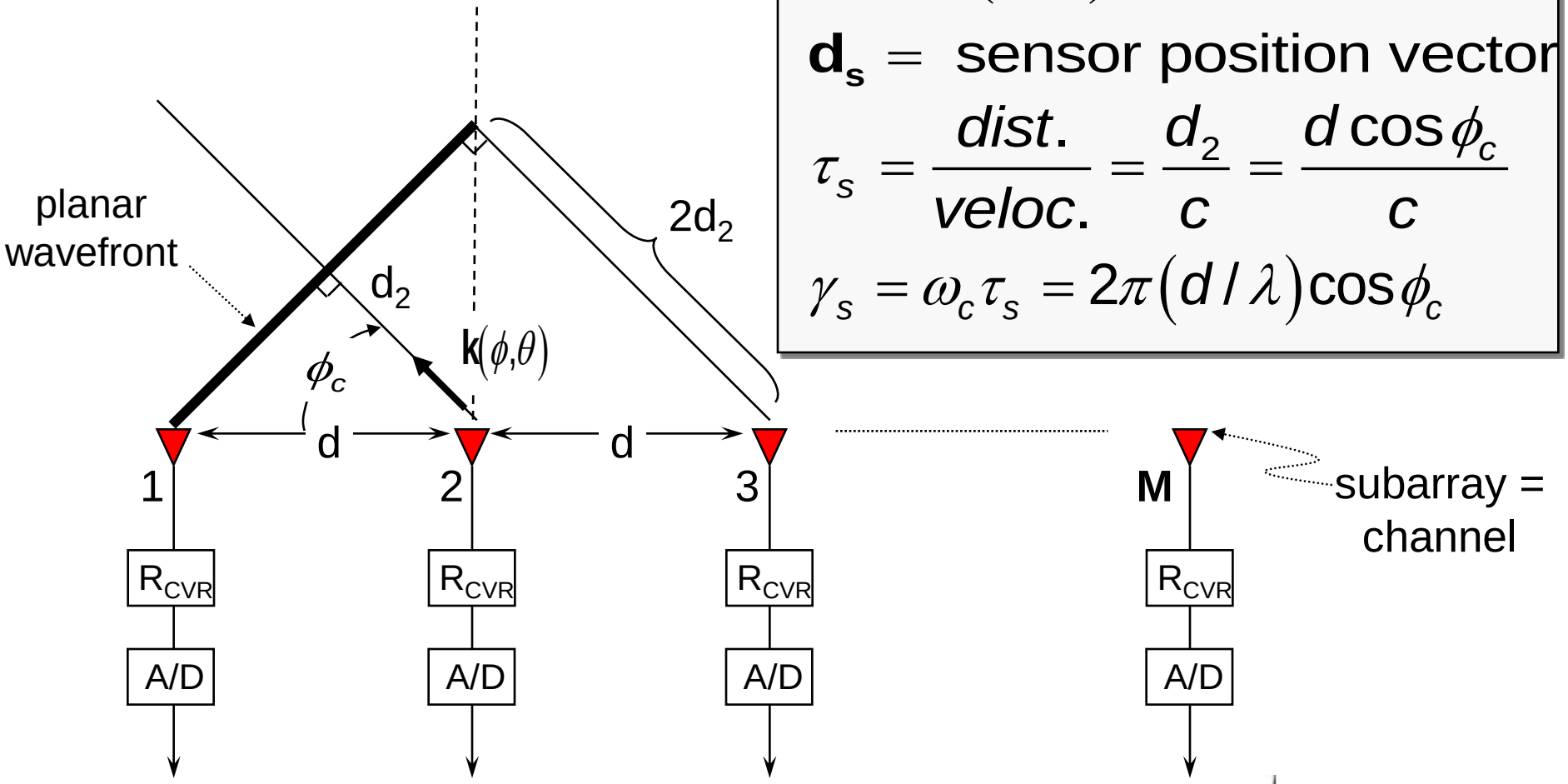

ϕ_c = cone angle

$d_2 = \mathbf{k}(\phi,\theta)\cdot\mathbf{d_s}$

$\mathbf{d_s}$ = sensor position vector

$$\tau_s = \frac{dist.}{veloc.} = \frac{d_2}{c} = \frac{d\cos\phi_c}{c}$$

$$\gamma_s = \omega_c\tau_s = 2\pi(d/\lambda)\cos\phi_c$$

Spatial Steering Vector

- Originally used to describe the spatial response of the array to signal with a specific direction of arrival (DOA)
  - The conjugate “steers” the beam
  - Terminology also used to describe temporal response
  - Matched filter

Spatial Steering Vector (uniformly-spaced linear array, or ULA)

$$\mathbf{s_s}(\gamma_s) = [1 \quad e^{j\gamma_s} \quad e^{j2\gamma_s} \quad \ldots \quad e^{j(M-1)\gamma_s}]^T \quad \left(= \mathbf{v_s}(\gamma_s)\right)$$

Maximum Signal-to-Noise Ratio (SNR) Filter
(a.k.a. Matched Filter)

Signal and noise snapshots: $\mathbf{s}, \mathbf{x_n} \in C^{Mx1}$

Uncorrelated noise signal: $\mathbf{n} \sim CN(\mathbf{0}, \mathbf{R_n})$; $\mathbf{R_n} = \sigma_n^2 \mathbf{I_M}$

$$SNR = \frac{P_s}{P_n} = \frac{E\left[y_s y_s^*\right]}{E\left[y_n y_n^*\right]} = \frac{E\left[\mathbf{w}^H \mathbf{s}\mathbf{s}^H \mathbf{w}\right]}{E\left[\mathbf{w}^H \mathbf{x_n}\mathbf{x_n}^H \mathbf{w}\right]} = \frac{\mathbf{w}^H \mathbf{R_s} \mathbf{w}}{\mathbf{w}^H \mathbf{R_n} \mathbf{w}}$$

$$= \frac{\sigma_s^2}{\sigma_n^2} \frac{\left|\mathbf{w}^H \mathbf{s_s}\right|^2}{\mathbf{w}^H \mathbf{w}} \leq \frac{\sigma_s^2}{\sigma_n^2} \frac{\left(\mathbf{w}^H \mathbf{w}\right)\left(\mathbf{s_s}^H \mathbf{s_s}\right)}{\mathbf{w}^H \mathbf{w}}$$

Achieves the upper bound when $\mathbf{w} = \mu \mathbf{s_s}$...

$$SNR = \left(\frac{\sigma_s^2}{\sigma_n^2}\right) M$$

Single Channel SNR

Integration Gain

Narrowband Jammer Signal

- Corrupts reflected signals with noise-like waveform occupying at least part of the victim radar receive bandwidth
  - Spatially correlated, generally white in slow-time

n = pulse number

T_p = PRI

Jammer waveform — Spatial steering vector

$$\mathbf{x_J}(nT_p) = w(nT_p)\,\mathbf{s_s}(\gamma_s)$$ (jammer spatial snapshot)

$$E\left[w(nT_p)w^*(mT_p)\right] = \sigma_J^2\ \delta((n-m)T_p)$$ (waveform correlation)

$$\mathbf{R_J} = \sigma_J^2\ \mathbf{s_s}(\gamma_s)\mathbf{s_s^H}(\gamma_s)\ \in\ C^{MxM}$$ (jammer ***spatial*** covariance matrix)

σ_J^2: Single channel/single pulse jammer power

$$\mathbf{R_{s\text{-}t/J}} = E\left[\begin{bmatrix}\mathbf{x_J}(0)\\ \vdots \\ \mathbf{x_J}((N-1)T_p)\end{bmatrix}\left[\mathbf{x_J^H}(0)\ \cdots\ \mathbf{x_J^H}((N-1)T_p)\right]\right] = \mathbf{I_N}\otimes\mathbf{R_J}\in C^{NMxNM}$$

(jammer ***spatio-temporal*** covariance matrix)

Multiple Jammers

- Assumption: Each jammer is statistically independent

$$\mathbf{x_J}(nT_p) = \sum_{m=1}^{P} \mathbf{x_{J;m}}(nT_p) \quad \Rightarrow \quad \mathbf{R_J} = \sum_{m=1}^{P} \mathbf{R_{J;m}}$$

- Each narrowband noise jammer requires a spatial DoF for cancellation
  - I.e., each resolvable narrowband jammer has rank of one in spatial domain

Objectives of Adaptive Digital Beamforming

- Processor selects adaptive weights to “optimize” performance
  - Maximizing SINR yields maximal probability of detection for a fixed false alarm rate [3, 4]
  - Minimizing output power subject to constraints [10]
    - Linear constraint on look-direction gain is most common
- Adaptive array reduces output colored-noise to boost detection performance to acceptable levels
  - Noise-limited scenario always provides an upper bound on performance
  - Signal diversity is the key to effective adaptive beamforming
    - Discriminate between target and interference responses
      - Spatial, slow-time, fast-time, polarization

Some Adaptive Array Highlights [12-13]

(**1957**) Paul Howells of GE, Syracuse (now Lockheed-Martin), develops technique to electronically scan antenna null in direction of a jammer

(1959) Howells receivers US Patent, "Intermediate frequency side-lobe canceller"

(1962) Howells and Sidney Applebaum successfully test five-loop side-lobe canceller

(1963) Howells and Applebaum, at Syracuse University Research Corp. (now Syracuse Research Corp.) investigate application of adaptive techniques to radar, including OTHR and BMD radar

(1965) Applebaum publishes "Adaptive Arrays," SURC TR-66-001, later available in IEEE Trans AP in 1976

(1969) Lloyd Griffiths publishes an adaptive algorithm for wideband antennas in Proc. IEEE

(1969) V. Anderson, H. Cox and N. Owsley separately publish works on adaptive arrays for sonar

(1971) R.T. Compton describes the application of adaptive arrays for communications systems in Ohio State Univ. Quarterly Rept. 3234-1, December 1971

(1972) O.L. Frost publishes an adaptive algorithm for antenna arrays incorporating constraints

(1972) Howells and Applebaum investigate adaptive radar for AEW

(**1973**) Brennan and Reed publish the seminal paper, "Theory of adaptive radar," in IEEE Trans. AES

(**1974**) Reed, Mallett and Brennan publish a paper describing the Sample Matrix Inverse (SMI) method for adaptive arrays in IEEE Trans. AES

(1976) "Adaptive antenna systems," published by Bernard Widrow et. al. in IEEE Proceedings

(1980) Monzingo and Miller publish the book Adaptive Arrays

(1983) Rule for calculating clutter subspace dimension proposed by Klemm in IEE Proc. Pt. F

(**1991**) Joint STARS prototypes deploy to Gulf War using adaptive clutter suppression methods (1978, Pave Mover was pre-cursor)

(1992) Klemm proposes spatial transform techniques

(1992) Real-time STAP implementation by Farina et. al.

(1994) Post-Doppler, beamspace method proposed by Wang and Cai in IEEE Trans. AES

(1994) Jim Ward of MIT Lincoln Lab summarizes STAP techniques in ESC-TR-94-109, *Space-Time Adaptive Processing for Airborne Radar*

(1998) Richard Klemm publishes first STAP text book, Space-Time Adaptive Processing: Principles and Applications

(1999) IEE ECEJ Special Issue on STAP (Klemm, Ed.)

(1999) STAP techniques for space-based radar, by Rabideau and Kogon, presented at IEEE Radar Conference

(1999) 3-D STAP for hot and cold clutter mitigation appears in IEEE Trans. AES by Techau, Guerci, Slocumb and Griffiths

(2000) Bistatic STAP techniques appear in literature (Klemm, Zatman and Kogon, Melvin et. al., Himed et. al.)

(2000) IEEE Trans. AES Special Section on STAP (Melvin, Ed.)

(2002) DARPA initiates Knowledge-Aided Sensor Signal Processing & Expert Reasoning Program aimed at advancing STAP (Guerci)

(2006) IEEE Trans. AES Special Section on Knowledge-Aided Sensor Signal and Data Processing (Guerci, Melvin)

(2006) MIMO radar (Bliss, Rabideau, Guerci, M. Davis, others)

Multiple Sidelobe Canceller (MSLC) [2, 10]

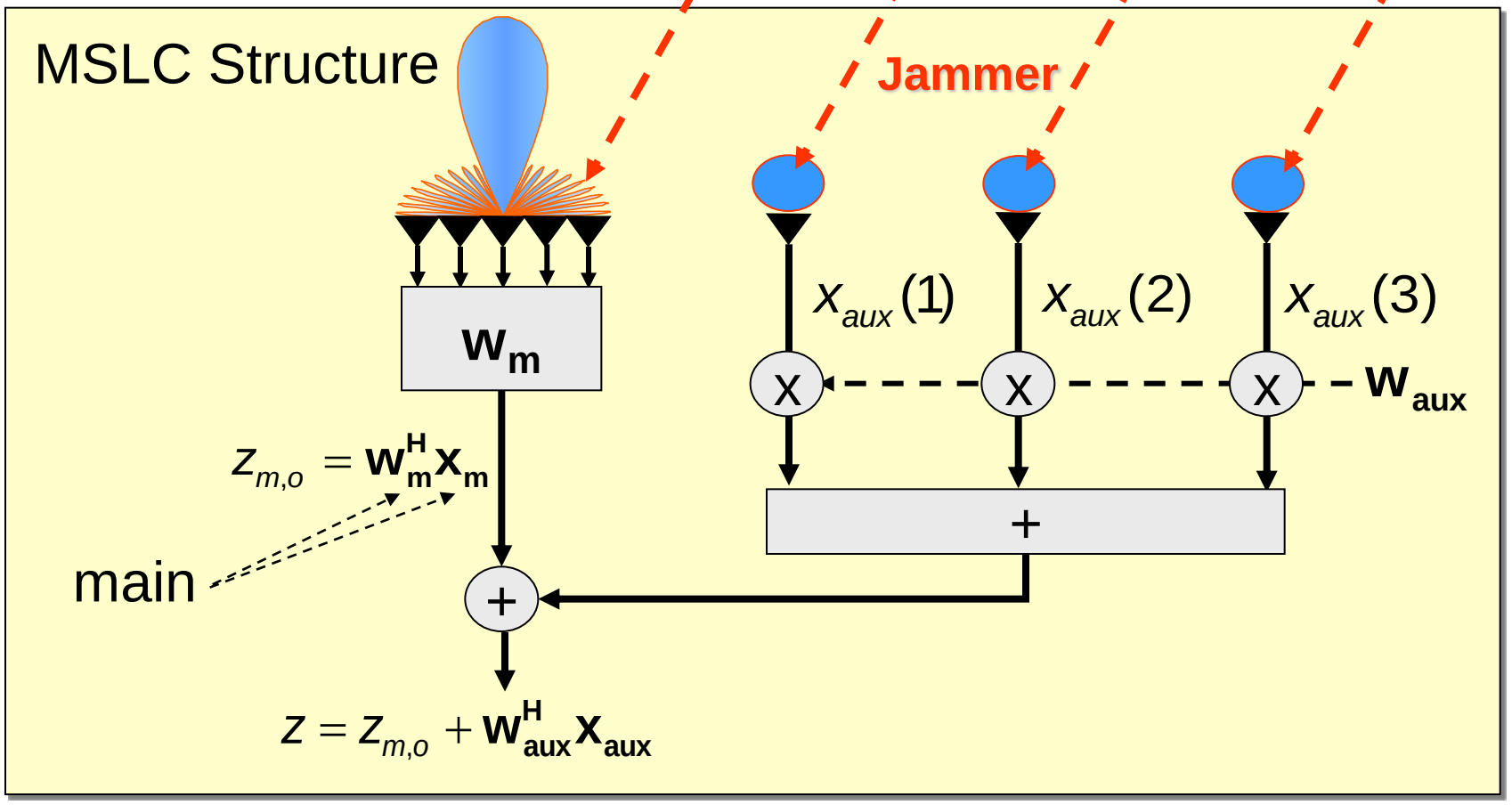

$$\mathbf{w}_{aux} = -\mathbf{R}_{aux}^{-1}\mathbf{r}_{aux\text{-}main}; \quad \mathbf{R}_{aux} = E\left[\mathbf{x}_{aux}\mathbf{x}_{aux}^H\right]; \quad \mathbf{r}_{aux\text{-}main} = E\left[\mathbf{x}_{aux}z_{m,o}^*\right]$$

The Maximum SINR Weight Vector [3-4]

Signal and I+N snapshots: $\mathbf{s}, \mathbf{x_n} \in C^{NMx1}$

Target signal: $\mathbf{s} = \alpha \mathbf{s_s}(\gamma_s)$; $\sigma_s^2 = E\left[\left|\alpha\, I\sqrt{2}\right|^2\right]$

Interference-plus-noise signal: $\mathbf{x_n} \sim CN(\mathbf{0}, \mathbf{R_n})$

$$SINR = \frac{P_s}{P_n} = \frac{E\left[y_s y_s^*\right]}{E\left[y_n y_n^*\right]} = \frac{E\left[\mathbf{w}^H \mathbf{s}\mathbf{s}^H \mathbf{w}\right]}{E\left[\mathbf{w}^H \mathbf{x_n}\mathbf{x_n}^H \mathbf{w}\right]} = \frac{\mathbf{w}^H \mathbf{R_s} \mathbf{w}}{\mathbf{w}^H \mathbf{R_n} \mathbf{w}}$$

$$= \sigma_s^2 \frac{\left|\tilde{\mathbf{w}}^H \tilde{\mathbf{s}}\right|^2}{\tilde{\mathbf{w}}^H \tilde{\mathbf{w}}} \le \sigma_s^2 \frac{\left(\tilde{\mathbf{w}}^H \tilde{\mathbf{w}}\right)\left(\tilde{\mathbf{s}}^H \tilde{\mathbf{s}}\right)}{\tilde{\mathbf{w}}^H \tilde{\mathbf{w}}}$$

$$\tilde{\mathbf{w}} = \mathbf{R_n}^{1/2} \mathbf{w}; \quad \tilde{\mathbf{s}} = \mathbf{R_n}^{-1/2} \mathbf{s_s}(\gamma_s)$$

Achieves the upper bound when $\tilde{\mathbf{w}} = \tilde{\mathbf{s}}$, or $\mathbf{w} = \mu \mathbf{R_n}^{-1} \mathbf{s_s}(\gamma_s)$...

$$SINR_{\max} = \sigma_s^2 \mathbf{s_s}^H \mathbf{R_n}^{-1} \mathbf{s_s}$$

Interpretation of Max. SINR Weight Vector

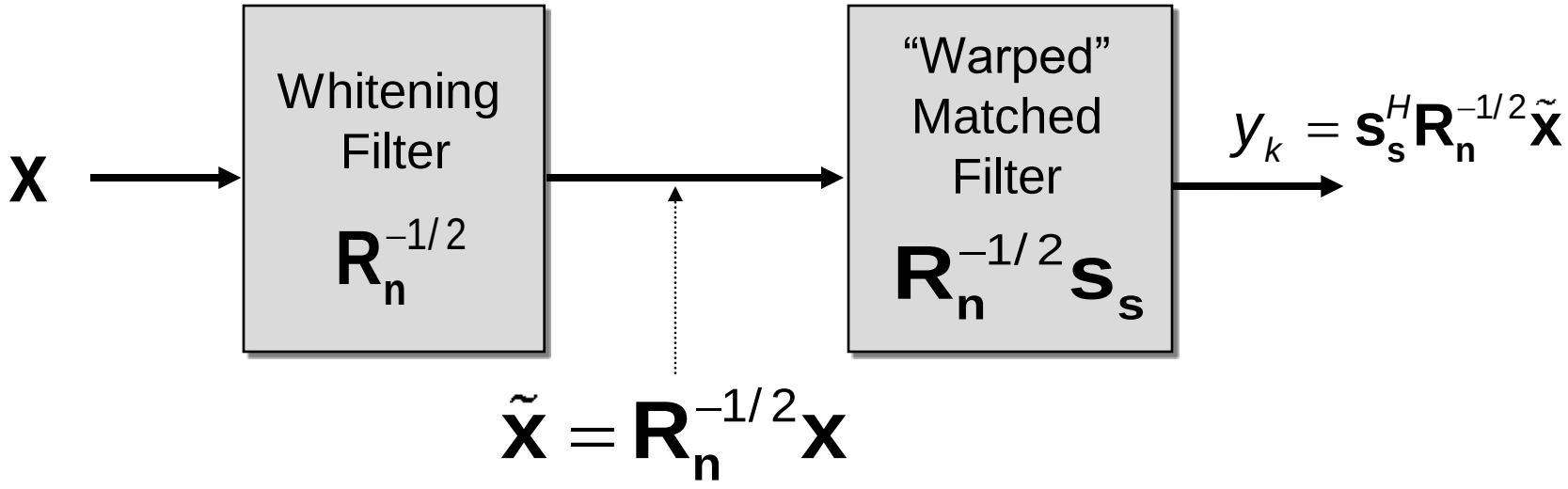

PSD of $\tilde{\mathbf{x}}$ appears white (flat over bandwidth):

$$E\left[\tilde{\mathbf{x}}\tilde{\mathbf{x}}^H\right] = \mathbf{R}_n^{-1/2} E\left[\mathbf{x}\mathbf{x}^H\right] \mathbf{R}_n^{-1/2} = \mathbf{R}_n^{-1/2}\mathbf{R}_n\mathbf{R}_n^{-1/2} = \mathbf{I}_M$$

$\mathbf{s}_s$ is the matched filter (noise-limited condition)

$\mathbf{R}_n$ is the interference-plus-noise covariance matrix

Minimum Variance Distortionless Response (MVDR) Spectra [2, 10]

- MVDR weight is proportional to maximum SINR weighting

$$y = \mathbf{w}^H\mathbf{x} \quad \rightarrow \quad \min_{\mathbf{w}} E\left[yy^*\right] \text{ subject to } \mathbf{w}^H\mathbf{s} = g \quad \Rightarrow \quad \mathbf{w}_{opt} = \frac{g^*\mathbf{R}^{-1}\mathbf{s}}{\mathbf{s}^H\mathbf{R}^{-1}\mathbf{s}}$$

- Minimum power at MVDR beamformer output is

$$P_{\min} = \mathbf{w}_{opt}^H\mathbf{R}\mathbf{w}_{opt} = \frac{1}{\mathbf{s}^H\mathbf{R}^{-1}\mathbf{s}}$$

- P_{min} is an estimate of the variance of $\boldsymbol{s}$
  - The MVDR beamformer passes the target signal, $\boldsymbol{s}$, with unity gain while minimizing power from other directions
- MVDR spectra follows by "sweeping" steering vector over all frequencies/directions of interest $S_{MVDR}(f_s) = \dfrac{1}{\mathbf{v}^H(\gamma_s)\mathbf{R}^{-1}\mathbf{v}(\gamma_s)}$
- MVDR spectra is a super-resolution spectra
  - Peaks sharper than traditional Fourier-based methods

Example MVDR Spectra

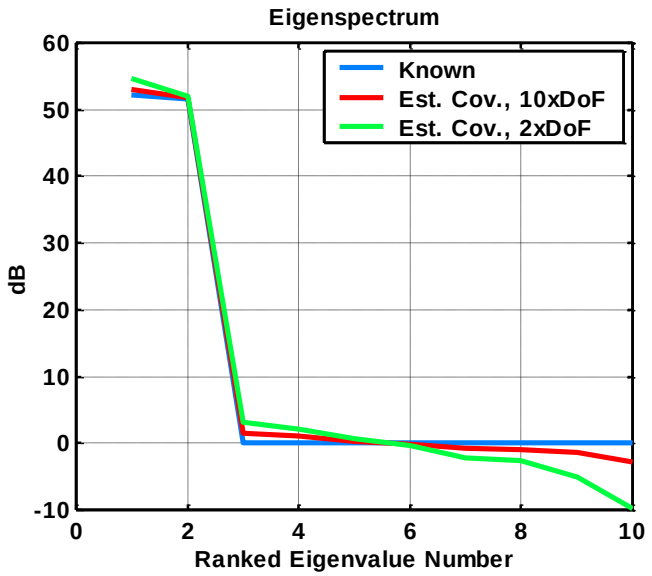

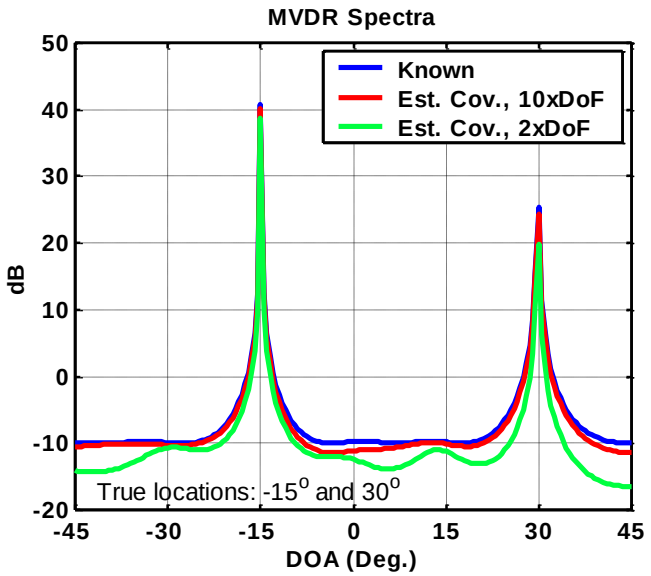

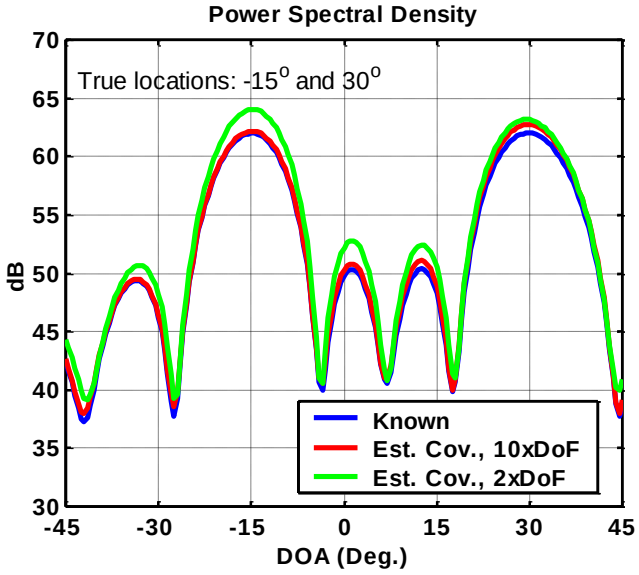

Generalized Sidelobe Canceler (GSLC) [14]

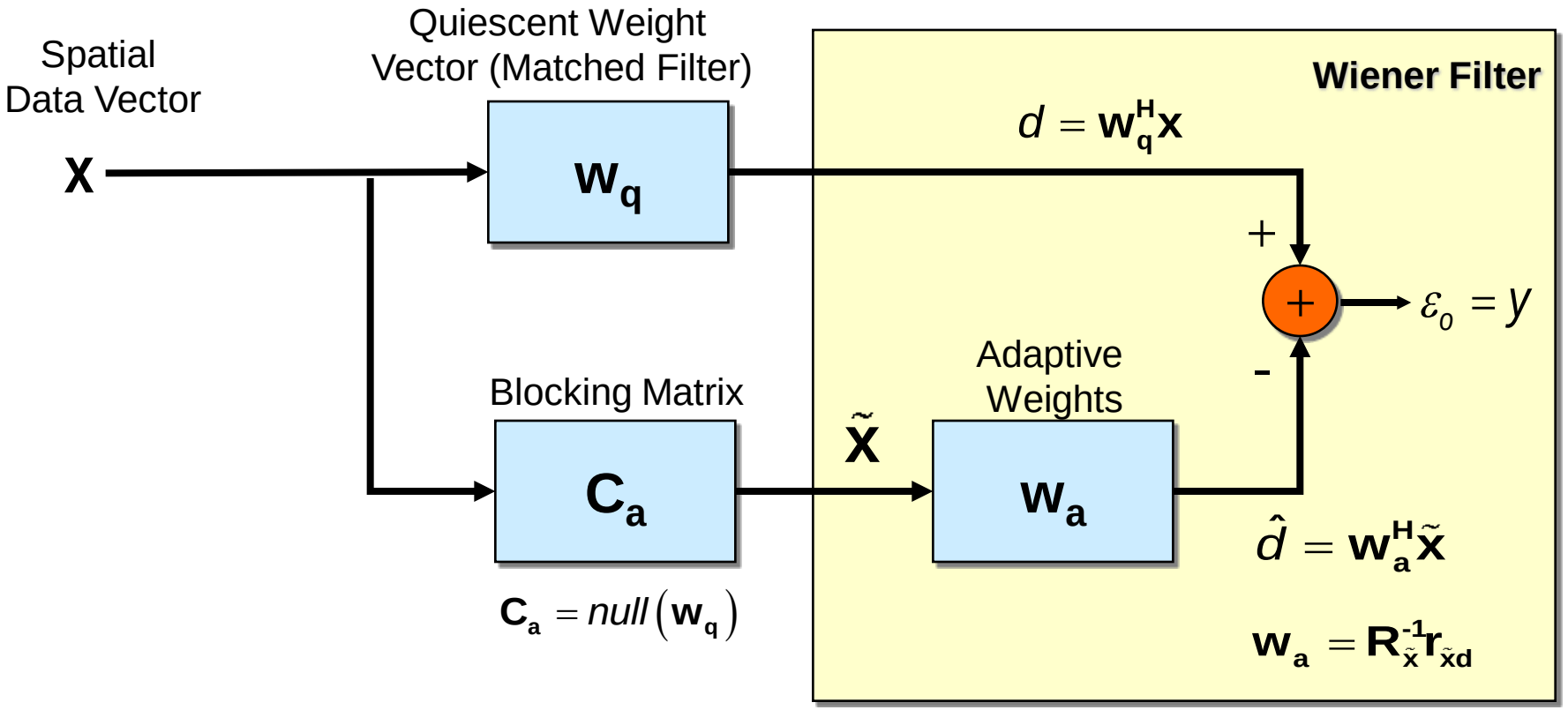

$d =$ desired response

$\hat{d} =$ estimate of colored noise portion of d

Orthogonal Projection [15]
(a.k.a., Principal Components Inverse)

$$\mathbf{R} = \sum_{m=1}^{NM} \lambda_m \mathbf{q_m} \mathbf{q_m^H}$$

For large components, $\lambda_m >> \lambda_0$...

$$y = \frac{\mathbf{s_s^H}(\gamma_s)}{\lambda_0}\left[\mathbf{I_M} - \sum_{m=1}^{P<<NM} \mathbf{q_m} \mathbf{q_m^H}\right]\mathbf{x} = \frac{\mathbf{s_s^H}(\gamma_s)}{\lambda_0}\tilde{\mathbf{x}}$$

$$\tilde{\mathbf{x}} = \left[\mathbf{I_M} - \sum_{m=1}^{P<<NM} \mathbf{q_m} \mathbf{q_m^H}\right]\mathbf{x} \overset{e.g.}{=} \mathbf{x} - a_1\mathbf{q_1} - a_2\mathbf{q_2}$$

$a_m =$ Karhunen-Loeve coefficients

- Above provides a basis for reduced-rank adaptive beamforming

Maximum Likelihood Estimate (MLE) [11]
(Reed, Mallett and Brennan (RMB) Rule)

$$\hat{\mathbf{R}} = \frac{1}{K}\sum_{m=1}^{K}\mathbf{x_m}\mathbf{x_m}^{H}$$

Assuming $\mathbf{x_m}$ are independent and identically distributed (*iid*) interference plus noise samples only:

$$\rho(\hat{\mathbf{R}}) = (\mathrm{SINR}\,|\,\hat{\mathbf{w}})/(\mathrm{SINR}_{\mathrm{Optimum}}) = \mathrm{L}_{s,2}$$

$$E[\rho(\hat{\mathbf{R}})] = (K+2-M_d)/(K+1)$$

$$M_d = \dim(\mathbf{x_m}) = \mathrm{M}$$

To be, on average, within 3dB of optimum:

$$K = 2M - 3$$

Substituting the covariance estimate yields the **Sample Matrix Inversion** (SMI) adaptive filter

Clairvoyant and Finite Sample Patterns

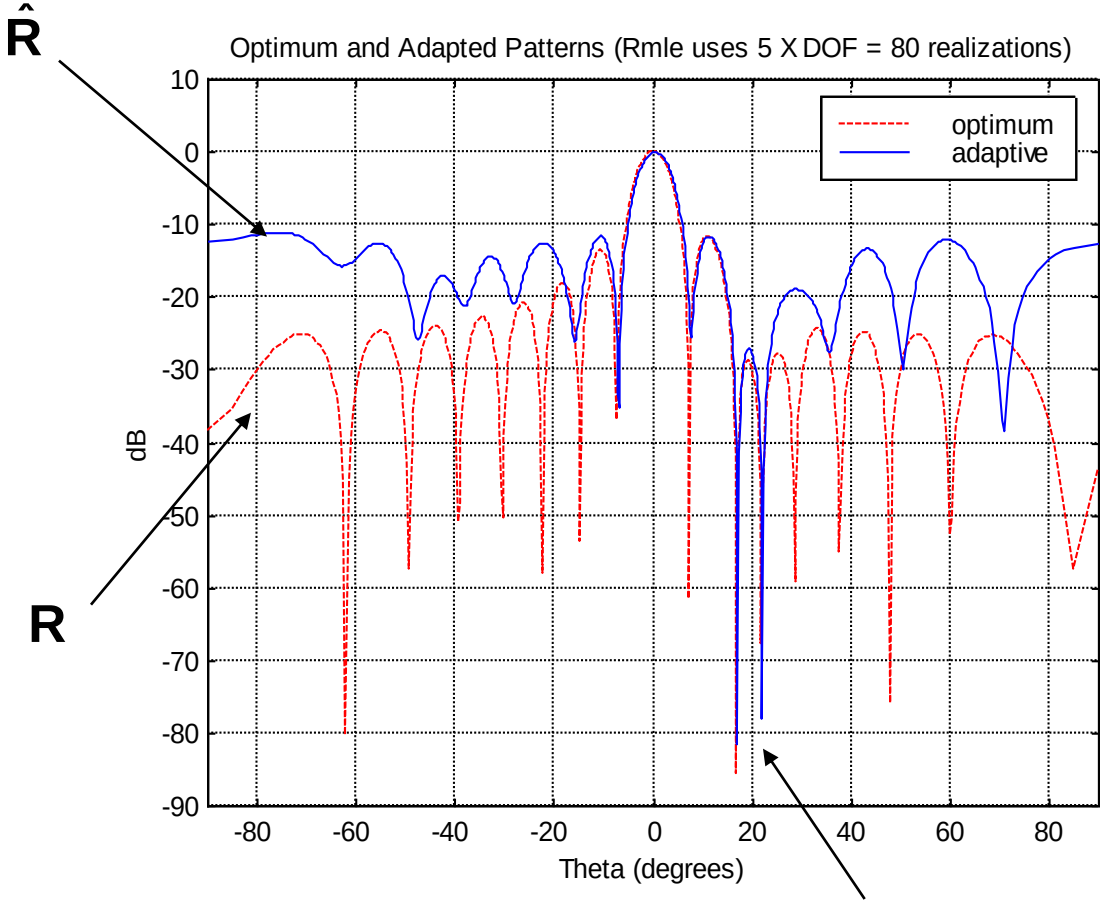

No diagonal loading

Jammers @ 17 and 23 degrees

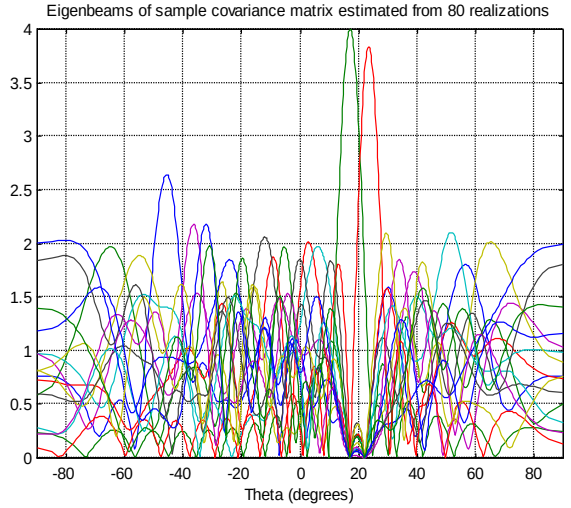

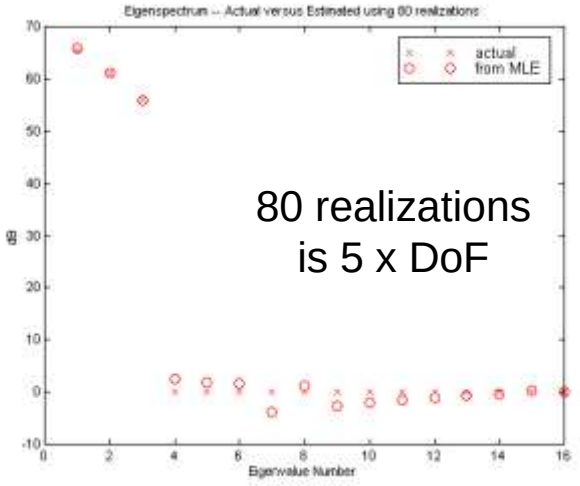

80 realizations is 5 x DoF

Georgia Institute of Technology

Pattern Synthesis [16]

$$\mathbf{R} = \sum_{m=1}^{NM} \lambda_m \mathbf{q_m} \mathbf{q_m}^H$$

$$\mathbf{w} = \frac{1}{\lambda_0}\left[\mathbf{s_s}(\gamma_s) - \sum_{m=1}^{NM} \frac{\lambda_m - \lambda_0}{\lambda_m} \alpha_m \mathbf{q_m}\right]$$

$$\alpha_m = proj\left(\mathbf{q_m}, \mathbf{s_s}(\gamma_s)\right)$$

$$y = \frac{\mathbf{s_s}^H(\gamma_s)}{\lambda_0}\left[\mathbf{I_M} - \sum_{m=1}^{NM} \frac{\lambda_m - \lambda_0}{\lambda_m} \mathbf{q_m} \mathbf{q_m}^H\right]\mathbf{x}$$

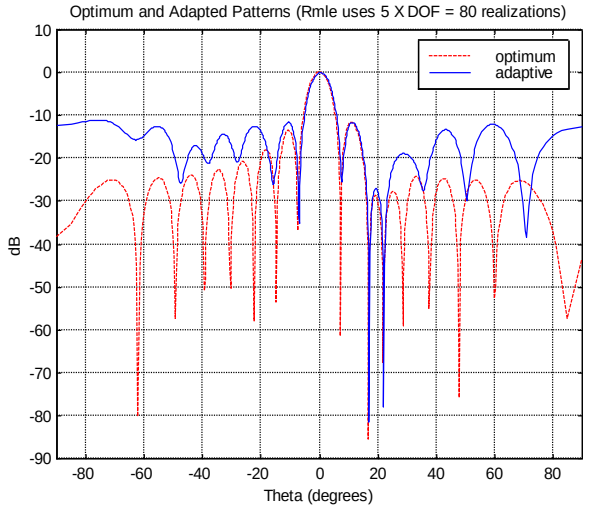

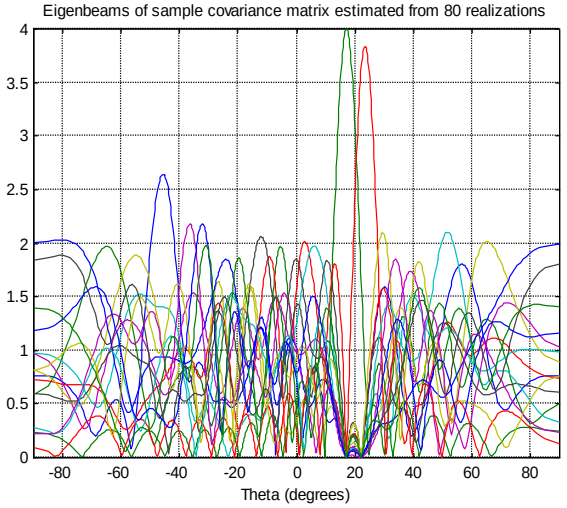

Hung-Turner Projection (HTP) [17]

- Given the snapshots...

$$\mathbf{x}(t_1) = \mathbf{j_1}(t_1) + \mathbf{j_2}(t_1) + \ldots + \mathbf{j_P}(t_1) + \mathbf{n}(t_1)$$
$$\mathbf{x}(t_2) = \mathbf{j_1}(t_2) + \mathbf{j_2}(t_2) + \ldots + \mathbf{j_P}(t_2) + \mathbf{n}(t_2)$$
$$\vdots$$
$$\mathbf{x}(t_P) = \mathbf{j_1}(t_P) + \mathbf{j_2}(t_P) + \ldots + \mathbf{j_P}(t_P) + \mathbf{n}(t_P)$$

- Use Gram-Schmidt to form the orthogonal basis $\{\mathbf{v_1}, \mathbf{v_2}, \ldots, \mathbf{v_P}\}$

(Notice $\mathbf{v_m} \in span\{\mathbf{j_1}, \mathbf{j_2}, \ldots, \mathbf{j_P}\}$)

- Form the weight vector $\bar{\mathbf{w}}_{\mathbf{Q}}^{\mathbf{o}} = \bar{\mathbf{w}}_{\mathbf{Q}} - \sum_{m=1}^{P} \left(\mathbf{v}_{\mathbf{m}}^{H} \bar{\mathbf{w}}_{\mathbf{Q}} \right) \mathbf{v_m}$

($\bar{\mathbf{w}}_{\mathbf{Q}}$ is the quiescent weight vector)

- Set the adaptive weight vector as $\bar{\mathbf{w}}_{\mathbf{A}} = \dfrac{\bar{\mathbf{w}}_{\mathbf{Q}}^{\mathbf{o}}}{\left\| \bar{\mathbf{w}}_{\mathbf{Q}}^{\mathbf{o}} \right\|_2}$

Beampattern Comparison

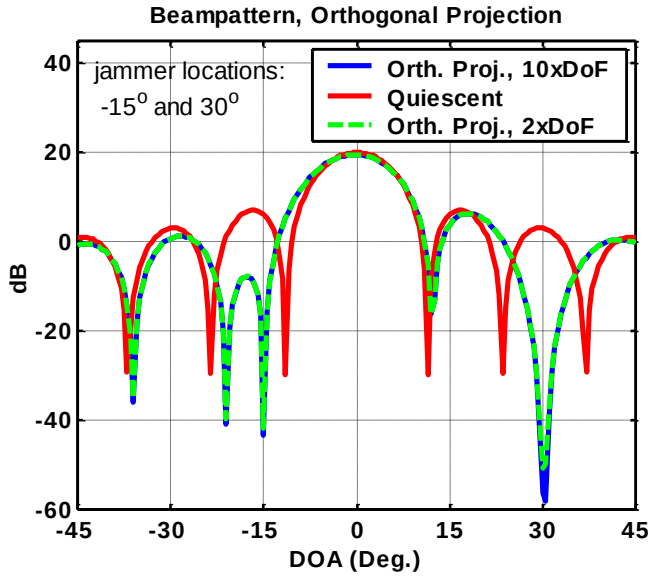

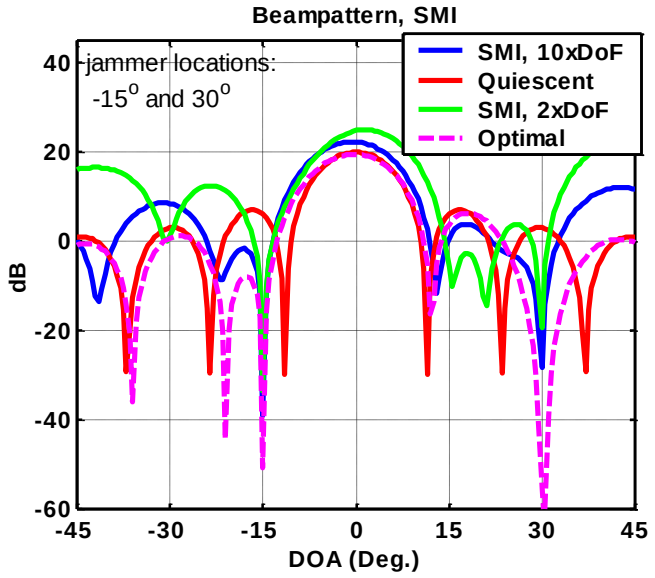

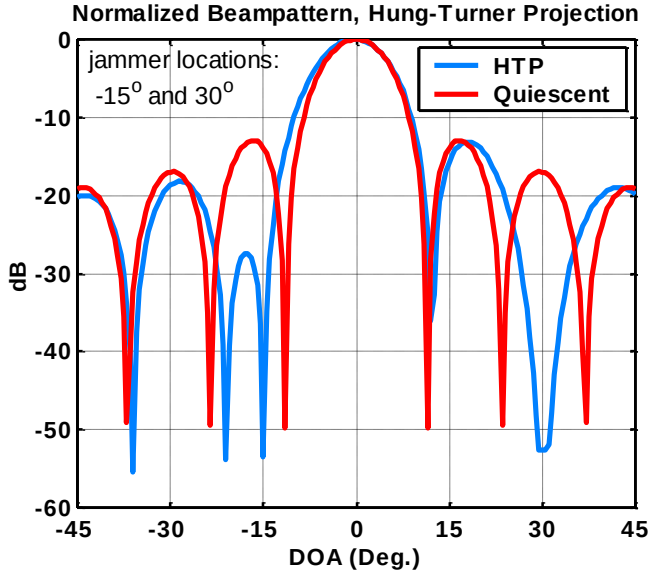

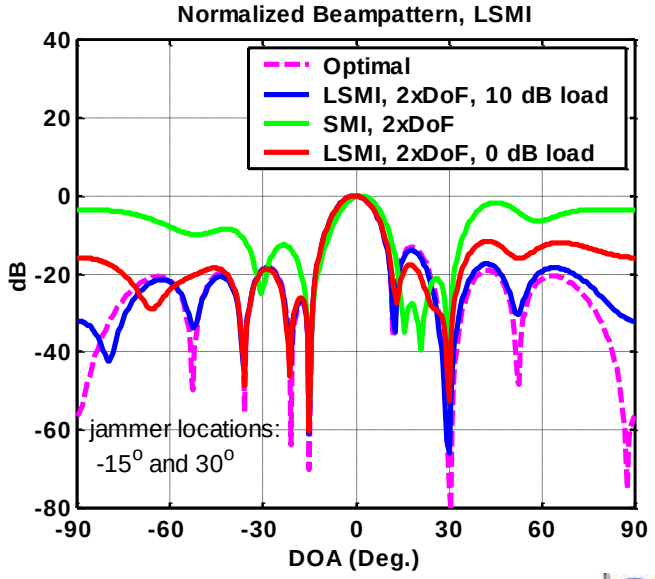

Wideband Effects

A single signal disperses across the array….appearing like multiple signals

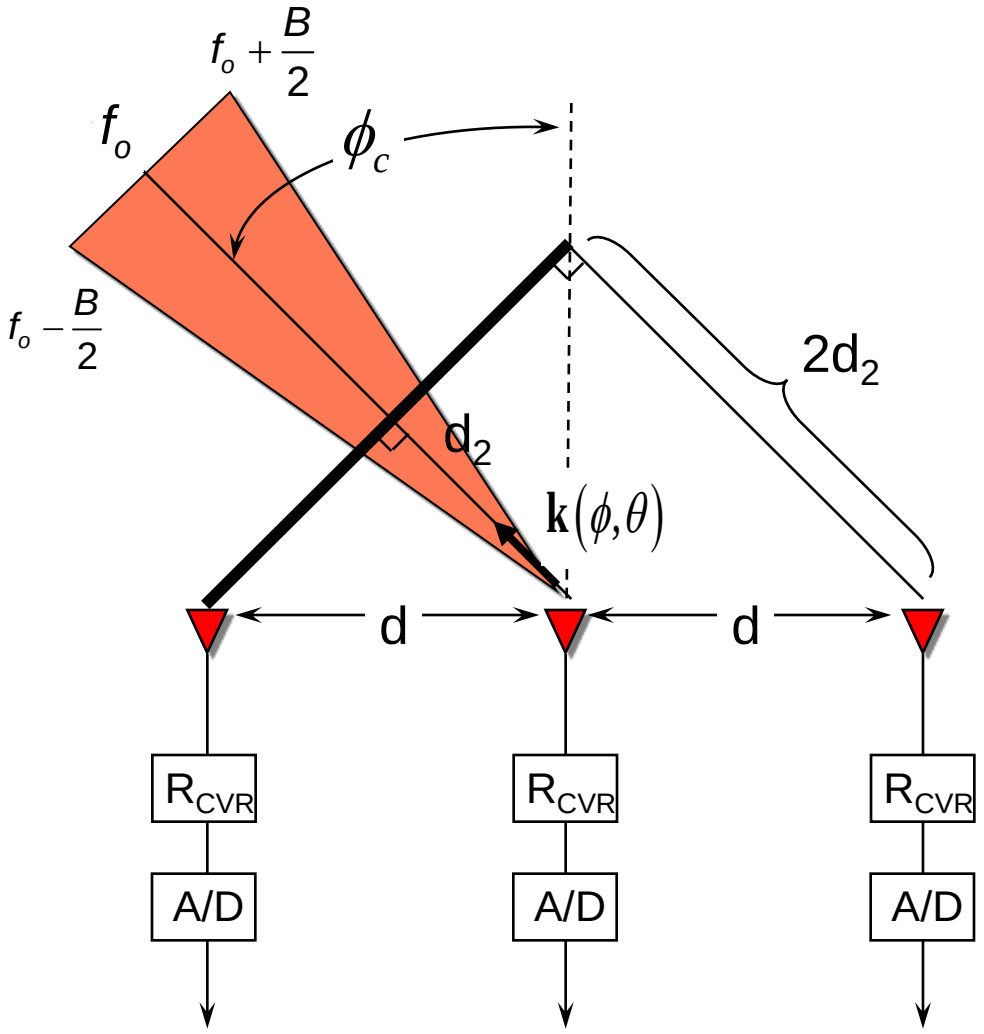

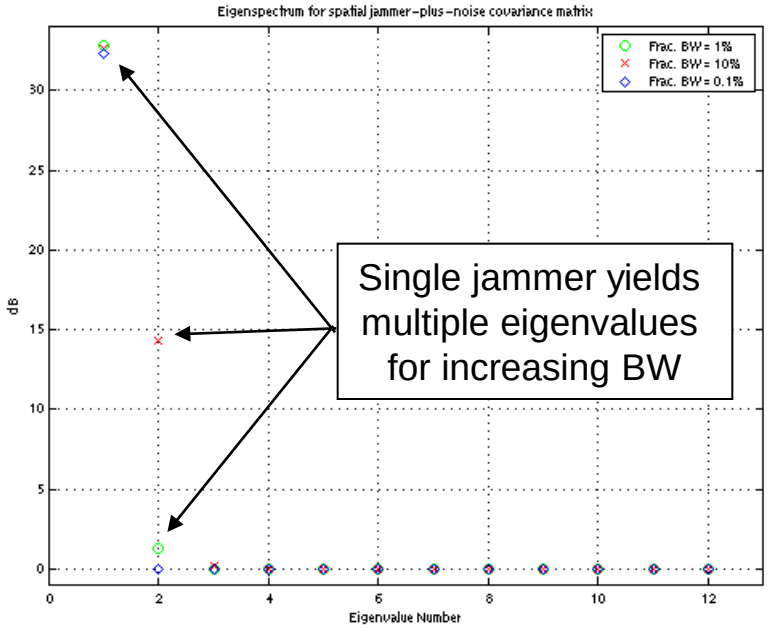

Single jammer yields multiple eigenvalues for increasing BW

$$\text{Time Delay} = \frac{\text{dist.}}{\text{veloc.}} = \frac{d_2}{c}$$

Phase = Time Delay x Radian Frequency

Wideband Beamforming Architecture [18-19] (Time Taps)

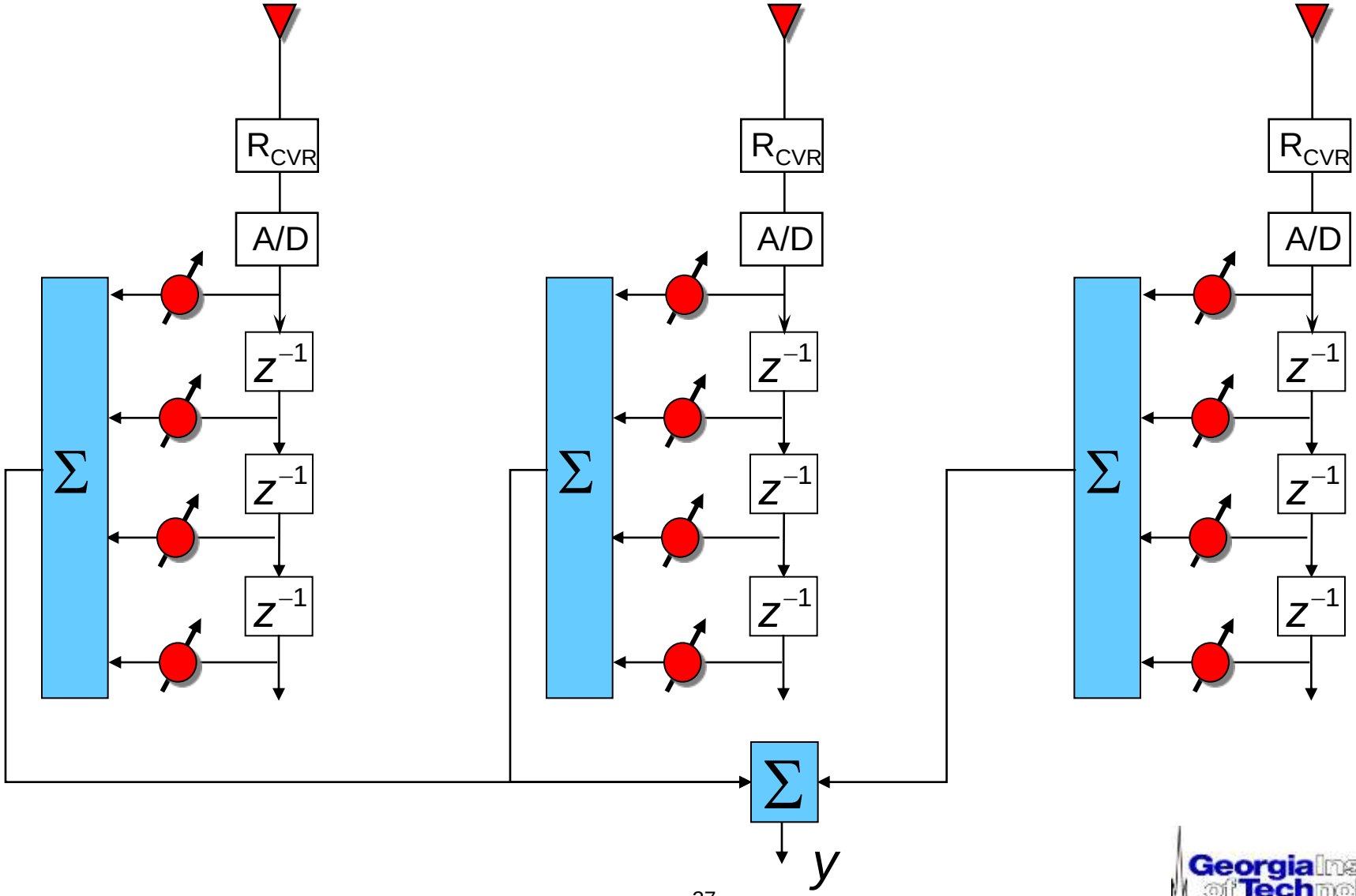

Wideband Cancellation Example

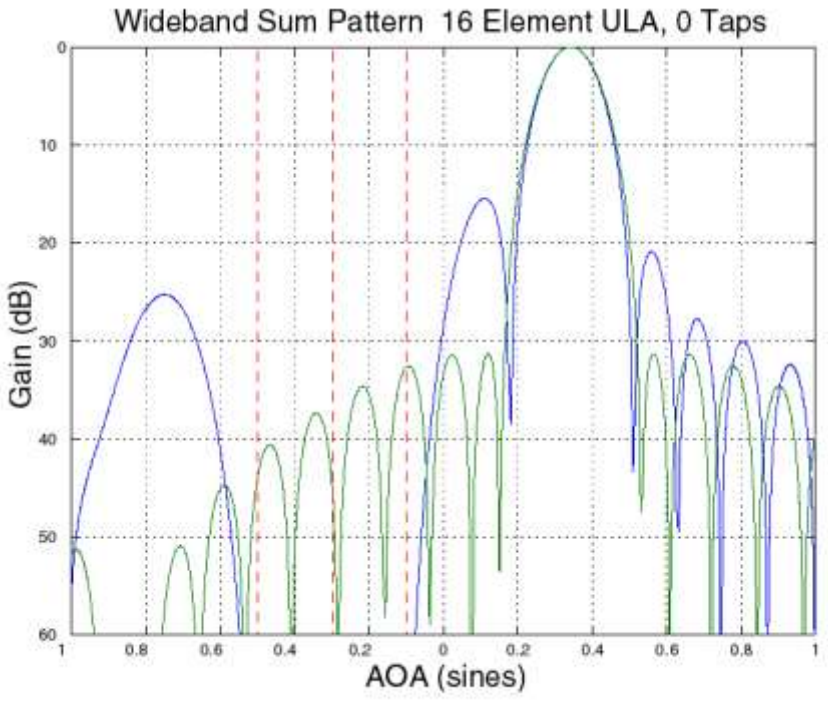

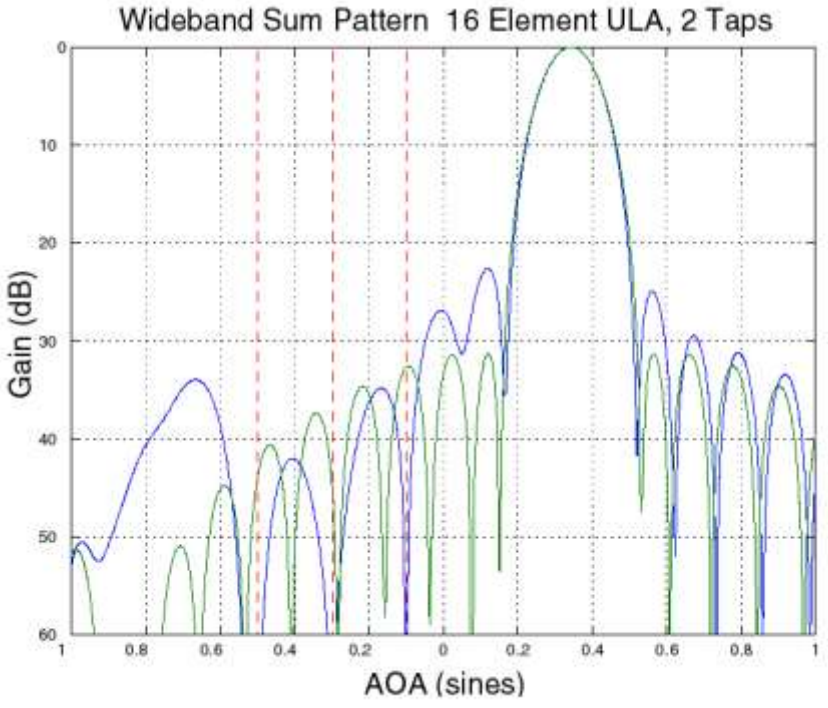

No Taps - One broad null cancels all three jammers

2 Taps - Sharp nulls on each jammer

* Compliments of Dr. David Aalfs, GTRI/SEAL

Wideband Beamforming Architecture (Sub-Banding)

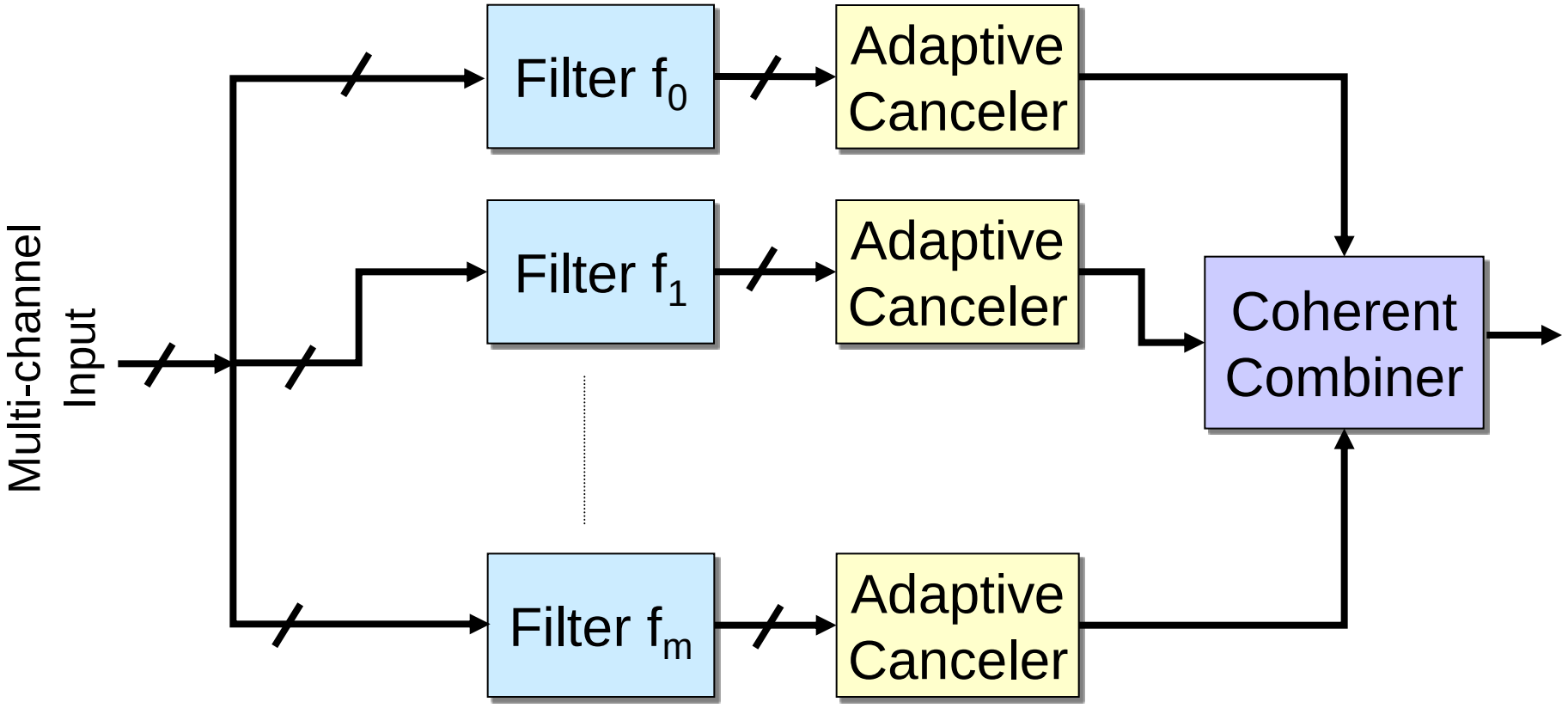

Solve *m* narrowband jammer cancellation problems and recombine

Summary

- Radar systems can employ sophisticated processing to enable detection and imaging over a range of operating conditions
- Focused on spatial nulling, but same ideas extend to other radar measurement spaces
  - E.g., multi-pass processing
  - E.g., Polarization STAP (P-STAP)
    - G.A. Showman, W.L. Melvin, M. Belen'kii, "Performance evaluation of two polarimetric space-time adaptive processing (STAP) architectures," in *Proceedings 2003 IEEE Radar Conference*, Huntsville, AL, 5-8 May 2003, pp. 59-65.
- Manipulating radar DoFs key to best detection and imaging performance
- Other cancellation strategies can be appropriate as source of interference varies

References

[1] M.I. Skolnik, Introduction to Radar Systems, 2nd Ed., McGraw Hill, New York, NY, 1980.

[2] D.H. Johnson and D.E. Dudgeon, Array Signal Processing: Concepts and Techniques, Prentice-Hall, Englewood Cliffs, NJ, 1993.

[3] J.V. DiFranco and W.L. Rubin, Radar Detection, Artech-House, Dedham, MA, 1980.

[4] L.E. Brennan and I.S. Reed, "Theory of adaptive radar," *IEEE Trans. AES*, Vol. 9, No. 2, March 1973, pp. 237-252.

[5] R. Klemm, Space-Time Adaptive Processing: Principles and Applications, IEE Radar, Sonar, Navigation and Avionics 9, IEE Press, 1998.

[6] J.R. Guerci, Space-Time Adaptive Processing for Radar, Artech House, Norwood, MA, 2003.

[7] W.L. Melvin, "A STAP overview," *IEEE AES Systems Magazine – Special Tutorials Issue*, Vol. 19, No. 1, January 2004, pp. 19-35.

[8] J. Ward, *Space-Time Adaptive Processing for Airborne Radar*, Lincoln Laboratory Tech. Rept., ESC-TR-94-109, December 1994.

[9] A.G. Jaffer, M.H. Baker, W.P. Ballance, J.R. Staub, *Adaptive Space-Time Processing Techniques For Airborne Radars*, Rome Laboratory Technical Rept. TR-91-162, July 1991.

[10] S. Haykin, Adaptive Filter Theory, Third Ed., Prentice-Hall, Upper Saddle River, NJ, 1996.

[11] I.S. Reed, J.D. Mallett, and L.E. Brennan, "Rapid convergence rate in adaptive arrays," *IEEE Trans. AES*, Vol. 10, No. 6, November 1974, pp. 853-863.

References (Continued)

[12] I.S. Reed, “A brief history of adaptive arrays,” Sudbury/Wayland Lecture Series (Raytheon Div. Education) Notes, 23 October 1985.

[13] R. Klemm, “Doppler properties of airborne clutter,” *Proc. Research and Technology Org., North Atlantic Treaty Org. (RTO-NATO) Lecture Series 228 – Military Applications of Space-Time Adaptive Processing*, RTO-ENP-027, September 2002, pp. 2-1—2-24.

[14] L.J. Griffiths and C.W. Jim, “An alternative approach to linearly constrained adaptive beamforming,” *IEEE Trans. AP*, Vol. AP-30, No. 1, January 1982, pp. 27-34.

[15] I.P. Kirsteins and D.W. Tufts, “Adaptive detection using low rank approximation to a data matrix,” *IEEE Trans. AES*, Vol. 30, No. 1, January 1994, pp. 55-67.

[16] W.F. Gabriel, "Using spectral estimation techniques in adaptive processing antenna systems," *IEEE Trans. AP*, Vol. 34, No. 3, March 1986, pp. 291-300.

[17] E.K.L. Hung and R.M. Turner, “A fast beamforming algorithm for large arrays,” *IEEE Trans. AES*, Vol. AES-19, No. 4, July 1983, pp. 598-607

[18] R.T. Compton, Adaptive Antennas: Concepts and Performance, Prentice-Hall, Englewood Cliffs, NJ, 1988.

[19] R.A. Monzingo and T.W. Miller, Introduction to Adaptive Arrays, John Wiley & Sons, New York, 1980.